Drazen Fabris[1]
e-mail: dfabris@scu.edu

Michael Rosshirt

Christopher Cardenas

Department of Mechanical Engineering,
Santa Clara University,
Santa Clara Center for Nanostructures,
Santa Clara University,
Santa Clara, California 95053

Patrick Wilhite

Toshishige Yamada

Santa Clara Center for Nanostructures,
Santa Clara University,
Santa Clara, California 95053

Cary Y. Yang
Department of Electrical Engineering,
Santa Clara University,
Santa Clara Center for Nanostructures,
Santa Clara University,
Santa Clara, California 95053

Application of Carbon Nanotubes to Thermal Interface Materials

Improvements in thermal interface materials (TIMs) can enhance heat transfer in electronics packages and reduce high temperatures. TIMs are generally composed of highly conductive particle fillers and a matrix that allows for good surface wetting and compliance of the material during application. Two types of TIMs are tested based on the addition of carbon nanotubes (CNTs): one mixed with a commercial TIM product and the other only CNTs and silicone oil. The materials are tested using an in-house apparatus that allows for the simultaneous measurement of temperature, pressure, heat flux, and TIM thickness. Results show that addition of large quantities of CNTs degrades the performance of the commercial TIM, while the CNT-silicone oil mixtures showed improved performance at high pressures. Thickness and pressure measurements indicate that the CNT-thermal grease mixtures are more compliant, with a small increase in bulk thermal conductivity over the range of tested pressures. [DOI: 10.1115/1.4003864]

Keywords: thermal interface materials, carbon nanotubes, thermal resistance

1 Introduction

Thermal interface materials (TIMs) are used in electronics packaging to increase heat conduction across the interface between two relatively flat surfaces. A good TIM will have both high conductivity and the ability to conform and contact the surfaces well [1]. There are a number of compositions of the TIM, but they typically involve mixtures of a highly conductive filler and a fluid carrier [2,3]. In some other cases, the TIM may also have the conductive paste on a metallic foil to stabilize the thickness of the material. The particle fillers are often highly conductive metals such as silver or copper particles. Performance of a TIM is based on the ability of the paste to flow and contact the surfaces in question while at the same time having very good contacts between the particle fillers that lead to the maximization of the conduction paths from surface to surface. A number of factors can limit the performance of TIM including poor wetting and contact of the surfaces at a microscopic level, incomplete or limited formation of conduction paths, and incomplete spreading across the surface to form a uniform thickness layer [3,4]. Furthermore, the surfaces' roughness and flatness characteristics can also factor into the ability of the TIM to spread across the surfaces.

A simple construction of the thermal resistance is based on the material bulk conductivity, bond line thickness, and contact resistances between the TIM and each surface

$$R''_{tc} = \frac{\mathrm{BLT}}{k_{\mathrm{TIM}}} + R_{c1} + R_{c2} \tag{1}$$

where R''_{tc} is the total TIM resistance, BLT is the bond line thickness, k_{TIM} is the TIM bulk conductivity, and R_{c1} and R_{c2} are the TIM to surface contact resistances [3]. The bond line thickness (BLT) is the surface to surface average separation accounting for asperities, surface roughness, and TIM to surface wetting. Even though this model is simple the parameters are sensitive to the thermal and rheological properties of the TIM, surface geometry, and TIM surface chemistry, in addition to the applied pressure and temperature at the interface. Contact resistance depends on the surface wetting of the TIM, which itself is dependent on the surface roughness and applied pressure, and the TIM surface chemistry or surface energy [5,6]. Contact resistance can also depend on the Kapitza resistance, which should be more significant at low temperatures ($<$100 K) and is not expected to dominate at room temperature [3,7].

Bond line thickness is the distance across which the conduction occurs and depends on the compliance of the TIM and the surface flatness and roughness [8]. Although the contribution of the surface compliance can be modeled [9,10], the TIM compliance is generally greater than the surface compliance. Both the surface roughness and the ability of the TIM to wet cavities have an impact on the effective conduction distance. Modeling has been done to estimate the effect of TIM non-Newtonian fluid properties, viscosity and shear stress, and chemistry to predict the penetration of the TIM into the surface cavities [3,5,6]. For the present work, the thermal surface flatness and roughness are small relative to the TIM thickness and the bond line thickness can be approximated as the thickness of the TIM itself.

The bulk TIM thermal conductivity depends on the composition of the TIM mixture. The conductivity of the filler particles, the matrix, and the particle to matrix resistance affects the bulk conductivity. Furthermore, the concentration or fraction of the filler particles will lead to different regimes of conduction. At low particle fraction the filler particles improve the conductivity through Maxwell's model for conduction through spherical included domains [11]. As the particle fraction increases, the particles may generate a percolation path for heat transfer, which will increase the conductivity over the Maxwell model [12]. As the fraction is further increased multiple conduction paths are established but the

[1]Corresponding author.

Contributed by the Electronic and Photonic Packaging Division of ASME for publication in the JOURNAL OF ELECTRONIC PACKAGING. Manuscript received December 6, 2009; final manuscript received February 18, 2011; published online June 7, 2011. Assoc. Editor: Cemal Basaran.

packing of the filler particles becomes an issue. An excellent review of the different phenomena is given in Prasher [3].

The present work investigates the use of carbon nanotubes as components to TIM. Carbon nanotubes (CNTs), carbon nanofibers (CNFs), and graphene sheets have strong potential for application in TIM due to their inherent high thermal conductivity [13]. CNTs and CNFs have advantages due to the high aspect ratio, typically 20–100 nm in diameter and several microns long. Even though the filler material may have a high conductivity, on the order of 100 W/m K, the effective conductivity of the TIM is only on the order of 1–10 W/m K [4], and the overall performance of the TIM can vary due to the factors mentioned. CNTs have been tested in TIM materials [11,14]. Hu, Jiang, and Goodson tested 0–2.2% volumetric loading of CNT in a 40% Ni sphere based TIM to improve the onset of thermal percolation in the TIM. Xu and Fisher grew arrays of TIM directly on Silicon to improve conductivity and compliance. The current work focuses on high concentration and comparison of experimental data to commercial TIM materials. The current tests vary the CNT loading in a commercial TIM from 0.5% to 2.18% by weight, which is equivalent to volumetric percentages of 90.9–97.75% and atomic percentages of 4.6–19.6%. For a comparison TIM performance, the CNTs are also added to a silicone oil with concentrations from 2.48% to 15.91% based on weight.

Finally, many techniques have been used to test TIM performance from direct testing in computer systems [15] from the use of a standardized apparatus to transient heating techniques. In the present work, we chose to use an apparatus based on the ASTM D5470-06 standard [16]. This allows for steady-state testing in a configuration similar to typical TIM packaging applications with high accuracy and flexibility. In the testing apparatus, eight thermocouples are used to reduce uncertainty and a micrometer is used to estimate in situ TIM thickness. The apparatus also allows for variation in applied pressure and variation in temperature of the TIM.

2 Experiment

The experimental apparatus was designed and built to meet the ASTM D4570-06 test standard. A number of modifications have been made to improve the accuracy and reliability of the apparatus. Heat is conducted one-dimensionally through two cylindrical "meter" bars fabricated from high-strength aluminum alloy 7075 (thermal conductivity, $k = 130.0$ W/m K), one inch in diameter. The standard requires surfaces parallel to within 5 μm and a surface roughness of Ra16 microinches (0.4 μm). The actual root-mean-square surface roughness was measured at 0.115 μm using a Zygo white-light 3-D surface profiler. Four fine-gauge unsheathed K-type thermocouples are embedded in the center of each meter bar, eight total, to measure the thermal gradient along the meter bar. The two additional thermocouples per meter bar provide a factor of redundancy to the temperature data in order to help diminish possible error caused by the thermocouple or insertion uncertainty and improve the extrapolation of the surface temperature (Fig. 2). Each meter bar is surrounded by a seamless shroud of polytetrafluoroethylene (PTFE) Teflon insulation. The coupling between the upper and lower insulation pieces uses an overlapping joint whose juncture is offset from the location of the sample. The thermal gradient along the meter bars is generated by two 100 W cartridge heaters at the top of the upper meter bar and an air cooled pin fin heat sink at the bottom of the lower meter bar. A 6.35 mm thick aluminum guard heater, heated by the same primary heat source, surrounds the upper half of the assembly to decrease losses through the insulation and preserve 1-D heat conduction through the meter bars. A double-acting pneumatic cylinder at the top of the apparatus applies pressure to the system. The overall alignment of the system uses the rods and bearing of a commercial die press. The data acquisition and heater power control are through National Instruments hardware and LABVIEW software.

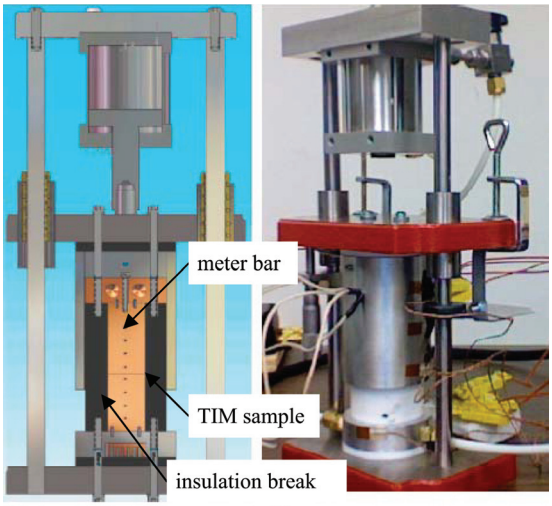

Fig. 1 (*a*) A cross-sectional view of the TIM apparatus revealing the meter bars shown centered in the lower half, the thermocouple holes along the center of the two meter bars, the heater holes above the upper meter bar, the insulation shroud (in black), the guard heater, and the heat sink beneath the lower meter bar, (*b*) TIM system assembly with micrometer for TIM thickness measurements

A Micro-Controle SM-25 micrometer with Vernier resolution of 1 μm is used to measure the working thickness of the TIM sample [Fig. 1(*b*)]. The micrometer measures the displacement of the upper half of the assembly when a thin TIM layer is applied at the interface. The thermal expansion and pneumatic compression offset of the system were calculated so that each micrometer measurement during a typical test could be properly scaled depending on the temperature of the system and the pressure applied.

Typically, the linear fit of the raw temperature data has a correlation coefficient, R^2 of 0.998. Due to heat losses and experimental uncertainties, the upper and lower heat rate values differ on average by 5% or less at steady state. The measurement of the

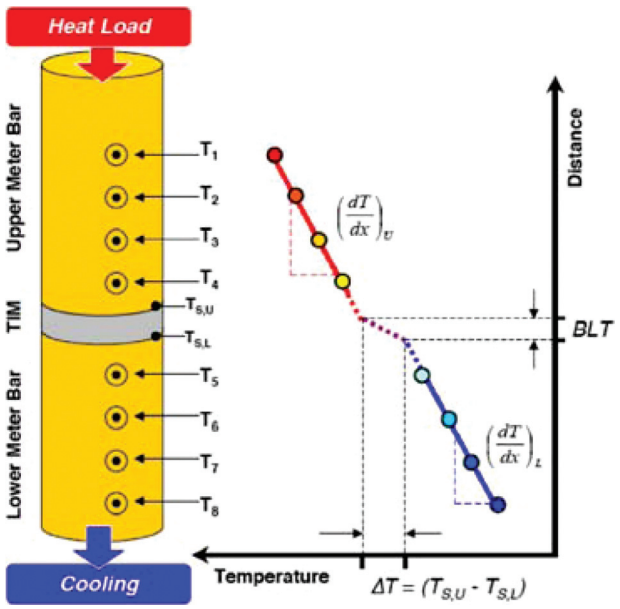

Fig. 2 The TIM apparatus measures R''_{tc} using eight K-type thermocouples to extract the thermal gradient along an upper and lower meter bar. The temperature drop at the interface is extrapolated from the gradient.

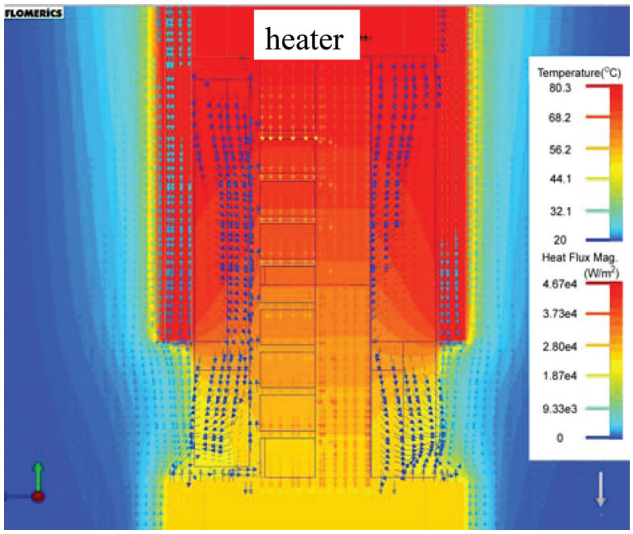

Fig. 3 FLOWTHERM simulation of the temperature profile through the test section of the TIM apparatus including the insulation and guard heater. The test section in the center shows 1-D conduction while the insulation and guard heater protect the system from radiation and convection losses.

thermal resistance requires a 10–20 min warm-up and reaches steady state after an additional 10 min. The measured resistance value is the average of two resistance values calculated using the upper and lower heat flux measurements separately.

Validation of the apparatus accuracy was done by two means. Bare surface to surface thermal conductivity was determined and compared to theoretical predictions. The measured surface contact resistance corresponded very well to the model prediction [10] over the range of pressures; results are provided in Rosshirt [17]. To determine the accuracy of the linear temperature gradient and the estimated heat flux, a numerical simulation of the apparatus was constructed using the commercial FLOWTHERM software (Mentor Graphics). In this simulation, the experimental thermocouple temperatures are used to extrapolate the boundary conditions at the top of the hot meter bar and the bottom of the lower meter bar. The simulation is then used to estimate the conduction losses to the sides and validated the essentially one-dimensional conduction through the meter bar. The simulated heat flux is compared to the experimental value and was found to vary by only 0.24%.

Calculation of the contact resistance depends on accurate calculation of the temperatures in the apparatus. Data were acquired for 20 s at 3 Hz and averaged for each measurement of temperature, and at steady state, measured temperatures vary by less than 0.02 °C. Heat loss through the top of the system and the guard heater contributes to 12% of the total power input with 88% going through the sample, while the modeled heat transfer through the sample and the experimentally calculated heat flux vary by 0.24%. The design stage uncertainty in the thermal resistance is 2.6% based on the thermocouple temperature uncertainty and variation in the recorded data. Including the additional thermocouples beyond the minimum required by the ASTM standard led to the low uncertainty. Scatter in the experiment indicates an uncertainty of 17.8% with 95% confidence in the thermal resistance. This scatter is attributed to variation in TIM thickness, h, partial misalignment of the heater bars, and a variation in pressure at the interface. The thermal interface thickness was measured with the micrometer to 1 μm resolution. The thickness measurement was calibrated for thermal expansion and pressure induced compression of the meter bars. The best estimate of thickness uncertainty is 10 μm while sample thicknesses vary from 45 to 90 μm. This results in some scatter in the R''_{tc}/h calculations. Misalignment and pressure variation were tested qualitatively with pressure sensitive paper and minimized as much as possible.

3 Performance Results With Arctic Silver® 5 and Carbon Nanotubes

The fundamental goal of this research is to improve the performance capabilities of TIM materials. Initial testing generated baseline data of a high performance industry standard TIM, Arctic Silver® 5 (AS). As a comparison, CNTs were introduced to the material as a simple experiment to identify their improvement. The CNTs, purified multiwall nanotubes with outer diameters ranging from 60 to 100 nm, were grown by SES Research and are available commercially. The TIMs were mechanically mixed using two parallel disks with the upper disk driven at 1500 rpm for a minimum of 30 min and then placed in an ultrasonic bath for approximately 45 min. Figure 4 shows as scanning electron microscopy image of the Arctic Silver®-Carbon nanotube mixture (CNT-AS). In introducing the CNTs, a high fraction was considered desirable. Previous work has shown that low fraction of CNTs can increase thermal conductivity of TIM materials [11]. In that work the upper limit of the improvement of thermal resistance had not been reached and the current experiments approach the material composition from the limit of high CNT content. Since CNT thermal conductivity is high, a high fraction of CNTs and thereby substitution of silver conductive paths with CNT elements should lead to an improvement in the performance. Test data are shown in Fig. 5 for several mass fractions of CNTs in the AS. The molecular weight of the CNTs is substantially less than the silver, and a small weight percentage corresponds to a high CNT volumetric fraction.

The experimental apparatus measures the temperature gradient in the meter bars and estimates the temperature jump across the TIM and the heat flux through the meter bars. From these two measurements, the overall thermal contact resistance, R''_{tc} can be measured as a function of the applied pressure to the system, shown in Fig. 5. The addition of CNTs generally reduced the performance of the mixture. The reduction in performance is directly related to the percentage of the included CNTs; hence, the higher the CNT fraction the greater the increase in overall thermal resistance. In the case of the lowest percentage of CNTs added, there is a small improvement at the highest pressure fraction (90 and 100 psi), but the improvement is within the uncertainty of the data. The second factor to notice in the experiments is the slope of the trend lines, which relate to an increase in compliance of the material, $R''_{tc} \alpha (1/p)^m$, where p is the applied pressure and m is a fitting constant. This is indicated by the increase in the magnitude of the

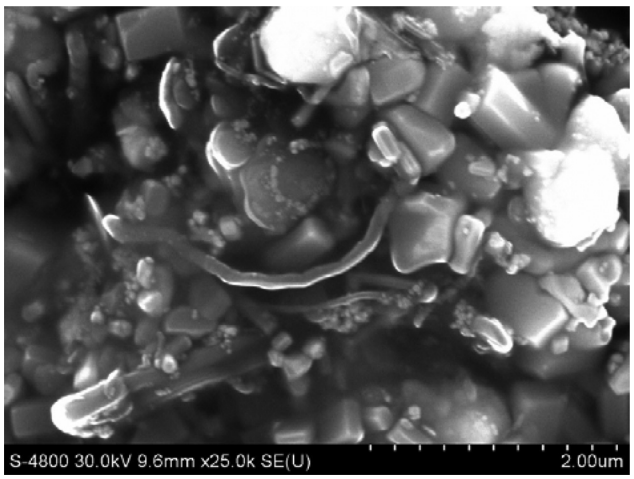

Fig. 4 Scanning electron microscope image of Artic Silver® 5 and CNTs. The mixture is composed of small (micron scale) silver particles and long submicron diameter CNTs visible as the curled tubes.

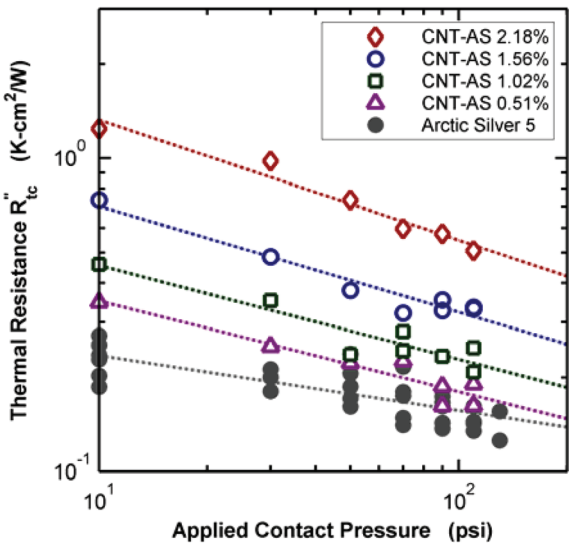

Fig. 5 Total thermal resistance per unit surface area, R''_{tc}, of Arctic Silver®5 and CNT TIM mixtures over the applied presure range. CNT inclusions changed the compliance of the TIM in all cases while the lowest percent weight fractions demonstrated the best thermal performance.

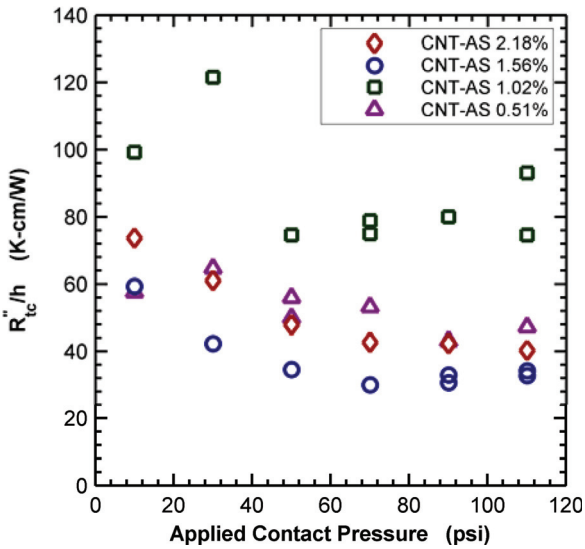

Fig. 6 Total thermal resistance per unit surface area relative to in situ sample thickness for CNT-AS mixtures. This quantity is inversely proportional to the mixture's bulk thermal conductivity.

negative slope with pressure, $m = 0.30$ to 0.38 for mixtures compared to 0.17 for AS. This behavior is more similar to the change in resistance of bare surfaces in contact [10,17] than a fully wetted paste between the surfaces. In applications some bonding pressure will be applied and the AS-CNT mixture can have reasonable performance characteristics; but unfortunately, very high bonding pressures may not be realistic in industrial applications.

From the measurements of overall thermal resistance and the thickness of the TIM, we can extract an estimate of the bulk thermal conductivity of the TIM, Eq. (1). Under the current experiments, the thickness of the sample is determined by measuring the initial position of the upper portion of the test apparatus with a micrometer prior to addition of the TIM. After the TIM is added the upper position is measured again and the difference is related to the TIM thickness, compression of the apparatus and possible thermal expansion of the apparatus. Using prior calibrations, the thickness measurement is adjusted for compression of the components in the apparatus and the thermal expansion during testing based on the interface temperature and the applied pressure load at the time of the measurement. This thickness is a first approximation of the bond line thickness. The tested thickness is on the order of 100–150 μm for the higher CNT concentration samples and 30–80 μm for the lower concentration mixtures, which is substantially larger than the variation due to the meter bar surface roughness (0.1 μm) and the surface flatness (<5 μm, but not experimentally characterized). In the current tests, surface contact resistances R_{c1} and R_{c2} are considered to be small relative to the contribution due to the BLT and thermal conductivity. The contact resistances and TIM to surface wetting are not measured directly and can contribute to the overall performance, but for the purpose of a sample to sample comparison of similar TIM materials R''_{tc}/h is directly calculated.

The thermal resistance per TIM thickness, shown in Fig. 6, is therefore an estimation of the bulk thermal conductivity of the paste (inversely related). The data show a relatively constant value over the pressure range with a slightly higher value of R''_{tc}/h at the lowest pressures. This corresponds to a lower bulk conductivity at the lower pressures and a constant value at the higher pressures. The mixture with the lowest concentration of CNTs has the most scatter and highest value because it is the thinnest TIM material and uncertainty in the thickness measurement contributes to this scatter. The uniformity of the data from R''_{tc}/h at high pressures indicates that the contact resistance may be small.

It is speculated that the initial higher resistance may be due to either a nonuniform initial spreading of the paste or microsized air bubbles trapped in the paste which with the increase in pressure are squeezed to a smaller size. The constant value also indicates that the high variation in total resistance with pressure seen in Fig. 5 can be attributed to a thinning of the material, which is consistent with the compression of small air bubbles or pump-out of excess material at the boundaries. A comparison of the different CNT fraction indicates a variation in bulk thermal conductivity of 30%. This is substantially lower than the order of magnitude variation in total thermal resistance shown in Fig. 5. The increase in thermal resistance with increasing CNT fraction is then mostly related to a thickening of the TIM material. This indicates that the high fraction of carbon nanotubes leads to a paste that is more difficult to spread and a less uniform and thicker initial layer. The Arctic Silver TIM thickness averaged 50 μm, while the average thickness of the CNT-AS mixtures varied between the CNT loadings from 140 μm for the 2.18%wt. CNT mixture to 35 μm for the 0.51%wt. CNT sample. The thicker paste also leads to speculation that microbubbles are trapped in the paste. Quantitatively, the estimate of bulk thermal conductivity of the paste is on the order of 2 W/m K, which is substantially lower than bulk silver or individual CNTs, but within the range of commercial TIMs [3].

4 Performance Results for Carbon Nanotubes in Silicon Oil

For the previous sets of experiments, it was determined that the performance of the CNTs should be directly isolated without additional particles, primarily silver in the commercial TIM. Therefore, a set of TIMs were created with CNTs mixed into a Dow Corning Fluid 200 silicone oil with 1000 cSt viscosity (CNT-oil). These mixtures again include high percent weight concentrations of CNTs and were mixed for a minimum of 30 min. followed by an ultrasonic bath for 45 min on average to generate uniformity based on visual and microscopic inspection. These mixtures exhibit better qualitative spreading characteristics than the CNT-AS. Experimental results of the overall contact resistance are shown in Fig. 7. The CNT-oil mixtures show better total thermal resistance performance than the CNT-AS mixtures. Similar to the previous tests, TIM also shows substantial compliance and reduction in overall resistance with the increase in pressure, $m = 0.49$ and 0.68 for the highest and two lower concentrations, respectively. In the

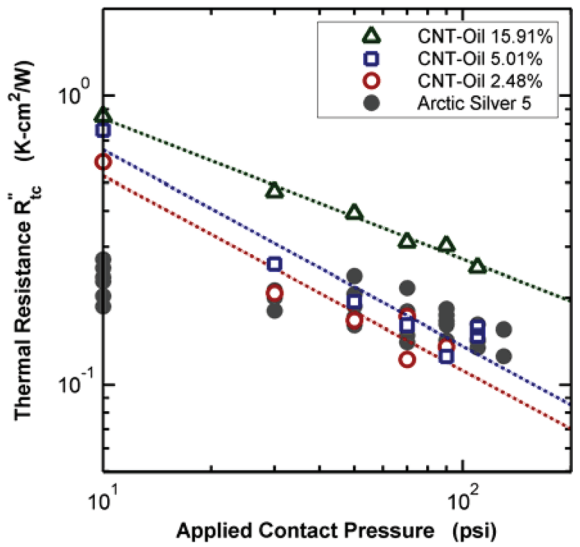

Fig. 7 Thermal contact resistance, R''_{tc} CNT, and silicone oil mixtures. No trend line is plotted for the Arctic Silver®5 data. CNT-oil mixtures show greater reduction in R''_{tc} with increasing pressure.

cases tested, two of the CNT/Oil mixtures at lower CNT fractions (2.48% and 5.01%) showed an improvement over the commercial TIM at the higher pressures (50 psi or greater). Rheological testing for a preliminary sample, 0.096% CNT, did not show an increase in viscosity, shear thinning, or viscoelastic behavior. Steady shear testing and oscillatory shear testing was done from 10^{-1} to 100 Pa by ATS Rheosystems.

In Fig. 8, the resistance is divided by the sample thickness. The data again show a strong collapse approaching a constant value. Consistently at lower pressure the resistance is greater indicating that there may be compression of bubbles or voids and an increase in the bulk conductivity of the mixture. This compression can also lead to an increase of the surface wetting of the TIM to the meter bars. Either of these effects would lower the value of R''_{tc}/h at high pressure. The CNT-oil mixtures also show better collapse among the different CNT fraction. This indicates that the thermal resistance may depend more on the TIM thickness and less on the CNT

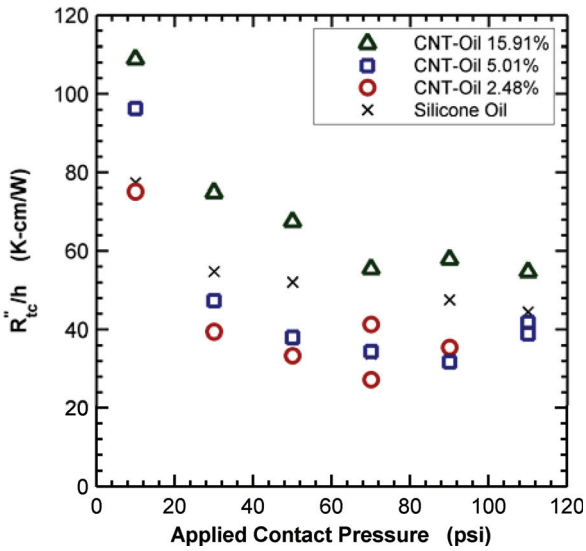

Fig. 8 Total thermal resistance per unit surface area relative to in situ sample thickness for the silicone oil and CNT TIMs. A greater reduction in resistance with thickness occurs at higher pressures.

fraction and bulk thermal conductivity. The bulk resistance test results display a variation of a factor of 7 while the resistance over thickness, R''_{tc}/h, measurements differ by 50%. Finally, comparing the CNT-oil mixtures to the Arctic Silver® 5 and the AS-CNT mixtures, we find that the thermal conductivity is comparable and the improvement in TIM resistance may be due to a reduced thickness. The values of R''_{tc}/h for this TIM and the CNT-AS TIM are comparable and inclusion of CNTs with or without the silver particles shows good thermal conductivity. Again, this performance is comparable to commercial performance and tested in a configuration similar to industrial applications.

5 Conclusions

Thermal interface materials are important for efficient removal of heat in electronics packaging applications. Improvement in TIM performance is dependent on developing materials that have both high thermal conductivity and high compliance. The introduction of CNTs into thermal interface materials has the potential for improving the bulk thermal conductivity. In preliminary testing, introduction of CNTs into a commercial TIM, Arctic Silver® 5, increases the thermal resistance and hence reduces the performance. At the same time, the CNT-AS mixtures show greater compliance. The performance change can be attributed to the increase in thickness due to difficulty in spreading the mixture. In a second test, a mixture composed of CNTs and silicone oil yields comparable or slightly improved performance over the CNT-AS mixture and the commercial TIM. The CNT/Oil mixture also shows high compliance and reduction of total resistance with increase in pressure. An estimate of the bulk thermal conductivity is found not to vary significantly with the fraction of CNTs in the mixture, displays little change with respect to pressure beyond an initial nominal loading, and is comparable to performance of commercial compounds.

Acknowledgment

This work was supported by the United States Army Space and Missile Defense Command (SMDC) and carries Distribution Statement A, approved for public release, distribution unlimited. The authors thank Kevin Lynch for initial TIM apparatus design work and Donald MacCubbin for manufacturing and design input.

References

[1] Gwinn, J. P., and Webb, R. L., 2003, "Performance and Testing of Thermal Interface Materials," Microelectron. J., **34**, pp. 215–222.
[2] Singhal, V., Seigmund, T., and Garimella, S. V., 2004, "Optimization of Thermal Interface Materials for Electronics Cooling Applications," IEEE Trans. Compon. Packag. Technol., **27**(2), pp. 244–252.
[3] Prasher, R., 2006, "Thermal Interface Materials: Historical Perspective, Status, and Future Directions," Proc. IEEE, **94**(8), pp.1571–1586.
[4] Misra, S., and Timmerman, J., 2009, "Thermally Conductive Liquid Materials for Electronics Packaging," IMAPS Advanced Technology Workshop on Thermal Management, Palo Alto, CA.
[5] Zhou, P., and Goodson, K. E., 2001, "Modeling and Measurement of Pressure-Dependent Junction-Spreader Thermal Resistance for Integrated Circuits," Proc. ASME, Heat Transfer Division, HTD, **369**(7), pp. 51–57.
[6] Prasher, R., 2001, "Surface Chemistry and Characteristic Based Model for the Thermal Contact Resistance of Fluidic Interstitial Thermal Interface Materials," ASME J. Heat Transfer, **123**, pp. 969–975.
[7] Cahill, D. G., Ford, W. K., Goodson, K. E., Mahan, G. D., Majumdar, A., Maris, H. J., Merlin, R., and Phillpot, S. R., 2003, "Nanoscale Thermal Transport," J. Appl. Phys., **93**(2), pp. 793–815.
[8] Prasher, R. S., 2004, "Rheology Based Modeling and Design of Particle Laden Polymeric Thermal Interface Materials," Thermomechanical Phenomena in Electronic Systems-Proceedings of the Intersociety Conference, Vol. 1, pp. 36–44.
[9] Yovanovich, M. M., and Marotta, E. E., 2003, "Thermal Spreading and Contact Resistances," *Heat Transfer Handbook*, A. Bejan and A. D. Krauf, eds., Wiley, New York.
[10] Mikic, B. B., 1974, "Thermal Contact Conductance: Theoretical Considerations," ASME J. Heat Transfer, **17**, pp. 205–214.
[11] Hu, X., Jiang, L., and Goodson, K. E., 2004, "Thermal Conductance Enhancement of Particle-Filled Thermal Interface Materials Using Carbon Nanotube Inclusions," Thermomechanical Phenomena in Electronic Systems-Proceedings of the Intersociety Conference, Vol. 1, pp. 63–69.

[12] Devpura, A., Phelan, P. E., and Prasher, R. S., 2000, "Percolation Theory Applied to the Analysis of Thermal Interface Materials in Flip-Chip Technology," Thermomechanical Phenomena in Electronic Systems-Proceedings of the Intersociety Conference, Vol. 1, pp. 21–28.
[13] Berber, S., Kwon, Y. K., and Tomanek, D., 2000, "Unusually High Thermal Conductivity of Carbon Nanotubes," Phys. Rev. Lett., **84**(20), pp. 4613–4616.
[14] Xu, J., and Fisher, T. S., 2004, "Thermal Contact Conductance Enhancement With Carbon Nanotube Arrays," Proc. ASME, Electron. Photonic Packag., EPP, **4**, pp. 559–563.
[15] Coles, O., 2009, "80-Way Thermal Interface Material Performance Test," Benchmark Reviews.com, Featured Reviews: Cooling, pp. 1–14.
[16] ASTM Standard D5470-06, 2006, "Standard Test Method for Thermal Transmission Properties of Thermally Electrical Insulation Materials," ASTM International, West Conshohocken, PA.
[17] Rosshirt, M., Fabris, D., Tu, T., Wilhite, P., and Yang, C. Y., 2009, "Comparison of Carbon-Based Nanostructures With Commercial Products as Thermal Interface Materials," Mater. Res. Soc. Symp. Proc., **1158**, pp. 37–42, 1158-F03-03.